ACS APPLIED MATERIALS & INTERFACES

Letter

www.acsami.org

Universal Fluorescence Biosensor Platform Based on Graphene Quantum Dots and Pyrene-Functionalized Molecular Beacons for Detection of MicroRNAs

Huan Zhang,[†,‡] Yunsheng Wang,[†,§] Daiwei Zhao,[†,§] Dongdong Zeng,[‡] Jiaoyun Xia,[⊥,∥] Ali Aldalbahi,[#] Chenguang Wang,[‡] Lili San,[‡] Chunhai Fan,[∥] Xiaolei Zuo,[*,∥] and Xianqiang Mi[*,‡]

[‡]Laboratory of System Biology, Shanghai Advanced Research Institute, Chinese Academy of Sciences, Shanghai 201210, China

[§]Thyroid Surgery, Second Affiliated Hospital of Guizhou Medical University, Kaili 556000, China

[⊥]School of Chemistry and Biology Engineering, Changsha University of Science and Technology, Changsha 410114, China

[∥]Division of Physical Biology and Bioimaging Center, Shanghai Synchrotron Radiation Facility, Shanghai Institute of Applied Physics, Chinese Academy of Sciences, Shanghai 201800, China

[#]Chemistry Department, King Saud University, Riyadh 11451, Saudi Arabia

Supporting Information

ABSTRACT: A novel biosensor platform was developed for detection of microRNAs (miRNAs) based on graphene quantum dots (GQDs) and pyrene-functionalized molecular beacon probes (py-MBs). Pyrene was introduced to trigger specifically fluorescence resonance energy transfer (FRET) between GQDs and fluorescent dyes labeled on py-MBs, and the unique fluorescent intensity change produced a novel signal for detection of the target. The platform realized detection of miRNAs in a wide range from 0.1 nM to 200 nM with great discrimination abilities, as well as multidetection of different kinds of miRNAs, which paved a brand new way for miRNA detection based on GQDs.

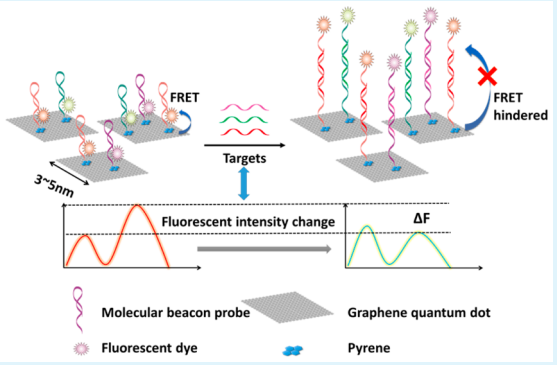

KEYWORDS: *biosensor, pyrene, graphene quantum dots, fluorescence resonance energy transfer, microRNA*

1. INTRODUCTION

It is of great importance to develop rapid, simple, sensitive, and selective biosensors for detection of proteins, nucleic acids, and other small molecules.[1,2] Molecular beacons (MBs) are elaborately designed stem-loop-structured oligonucleotides dual-labeled by a fluorophore and a quencher, which could be used as fluorescent probes for biomolecular detection with high sensitivity and excellent specificity.[3,4] MBs had explored wide applications in molecular biological studies, pathogen detection, and biomedical diagnostics.[5,6] Graphene quantum dots (GQDs) are nanometer-sized graphene fragments, where electronic transport is confined in all three spatial dimensions.[7,8] Because of the unique properties, GQDs have attracted great attentions in a wide range of new applications.[9] In particular, GQDs have shown promising prospects in bioimaging and biodetection fields due to their outstanding fluorescence performances.[10,11] In recent years, GQD-based fluorescent sensors have been widely studied. For example, it is first reported that GQDs could be used for Fe^{3+} detection on the basis of the selective fluorescence quenching ability of GQDs to Fe^{3+}.[7] Through luminescence resonance energy transfer (LRET) between graphene and GQDs, human immunoglobulin G (IgG) could be detected via a novel signaling transduction strategy.[12] It is well-known that graphene and its derivatives (such as graphene oxide) have wide applications in small molecular detection, especially in building "signal-on" fluorescent biosensors for analysis of nucleic acid molecules.[13−15] Although GQDs and graphene have similar hexagonal honeycomb lattice structures made of carbon atoms, there is not much research work utilizing GQDs to build fluorescent sensing platforms for detection of small nucleic acid molecules (especially DNA or miRNA). We assumed that because of instinct, small size, and electronegativity of GQDs, it might be difficult for small nucleic acid molecules (NAs) to combine through $\pi-\pi$ stacking interaction between the aromatic ring structures of nucleobases and the hexagonal cells of GQDs like they did with graphene, which greatly limited their applications.

Herein, we demonstrated a novel fluorescence biosensor platform based on graphene quantum dots (GQDs) and

Received: June 1, 2015
Accepted: July 22, 2015
Published: July 22, 2015

DOI: 10.1021/acsami.5b04773
ACS Appl. Mater. Interfaces 2015, 7, 16152−16156

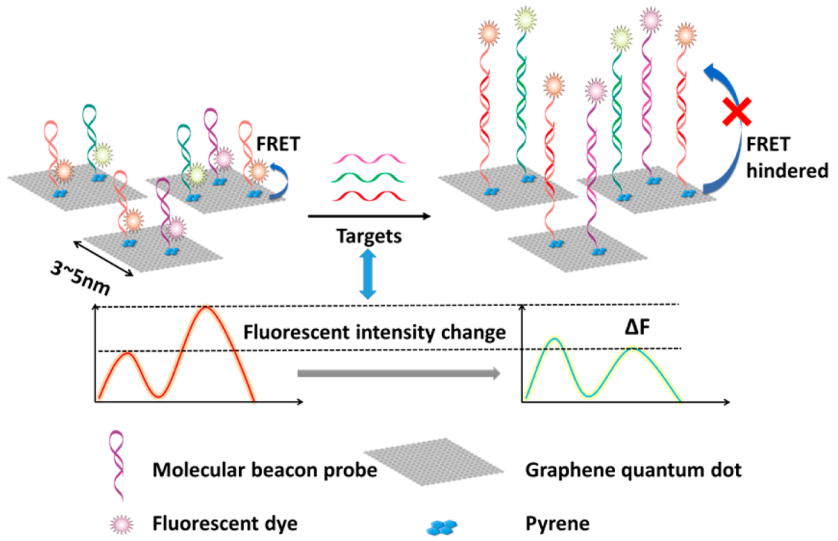

Figure 1. Schematic illustration of the novel biosensor platform based on FRET changes between graphene quantum dots and pyrene-functionalized molecular beacon probes for detection of miRNAs.

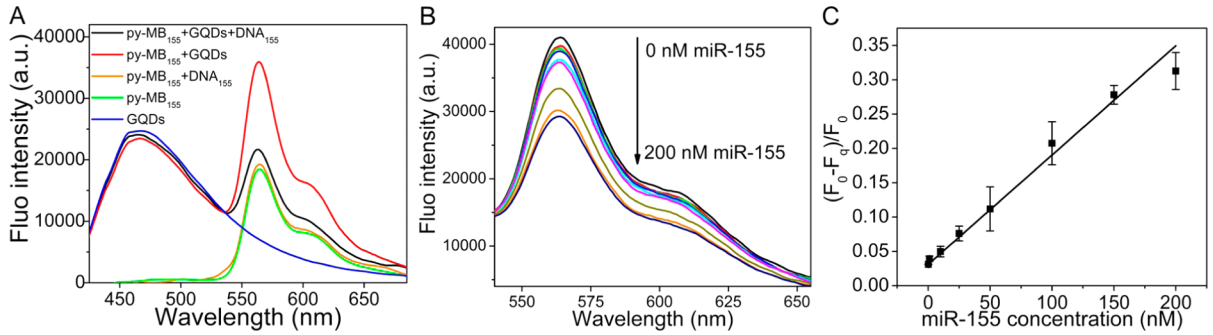

Figure 2. (A) Fluorescent spectrum illustrated the detection strategy of our biosensor platform. Fluorescent curves of GQDs (1.0 μg mL^{-1}, blue trace), the Cy3-labeled py-MB$_{155}$ probe alone (300 nM, green trace), py-MB$_{155}$ probe,and DNA$_{155}$ targets without GQDs (orange trace), GQDs and py-MB$_{155}$ probe biosensor system (red trace) and after incubation with DNA$_{155}$ target (black trace). (B) Fluorescence spectra of the biosensor after incubation with various concentrations of miR-155 (0, 0.1, 1, 10, 25, 50, 100, 150, and 200 nM), measured with excitation wavelength of 400 nm. (C) Linear relationship between the relative fluorescence signal change ΔF_r ($(F_0 - F_q)/F_0$) and the concentration of miR-155 target.

pyrene-functionalized molecular beacon probes (py-MBs). We took advantage of excellent fluorescence performance of GQDs, instinct base pairing specificity of MBs and unique fluorescence resonance energy transfer (FRET) from GQDs to fluorescent dyes labeled on py-MBs to realize qualitative and quantitative analysis of miRNAs. To the best of our knowledge, it is the first time that a GQD-based FRET biosensor platform was designed for detection of miRNAs. During our design, pyrene was introduced to guarantee the significant FRET between GQDs and fluorescent dyes labeled on MBs, generating an increased fluorescence signal. The hybridization between target miRNA and the loop structure of py-MBs then resulted in opening of the hairpin structures, forming more rigid duplexes structures, which significantly hindered the FRET and thus decreased the fluorescence signal of the fluorescent dyes. The fluorescent intensity changes of the dyes labeled on py-MBs produced a novel strategy for rapid analysis of miRNA targets. The novel platform exhibited good performance in quantitative detection of miRNA targets with great sensitivity and selectivity. Meanwhile, through choosing proper fluorescent dyes and changing the loop sequences of py-MBs, we realized simultaneously multidetection of different miRNAs.

2. RESULTS AND DISCUSSION

To realize efficient FRET, we elaborately designed our py-MBs with 5′ modification of pyrene and 3′ modification of selected fluorescent dyes (Cy3 or Cy5 in our work), leaving the sequence of the loop structures completely complementary to the miRNA targets. Pyrene is a well-known aromatic hydrocarbon with unique photophysical properties. It is reported that pyrene can be represented as a fragment of a graphene sheet, which could form a flat binding mode with graphene due to the $\pi-\pi$ stacking interaction.[16−18] Considering of the structure similarity between graphene and GQDs, we believed that pyrene could also strongly attach on the surface of GQDs by $\pi-\pi$ stacking interactions. Therefore, the introduction of pyrene would ensure that the py-MBs and GQDs were close enough to trigger FRET, generating an increased fluorescence signal of dyes labeled on probes. Upon the hybridization of the loop structure of py-MBs with the target miRNAs, the hairpin structures of py-MBs were opened and formed more rigid duplexes structures. The distance between the GQDs and fluorescent dyes increased which significantly hindered the FRET and decreased the fluorescence signal of the fluorescent dyes. The fluorescent intensity changes of fluorescent dyes produced a novel signal for detection of miRNA targets (as

DOI: 10.1021/acsami.5b04773
ACS Appl. Mater. Interfaces 2015, 7, 16152−16156

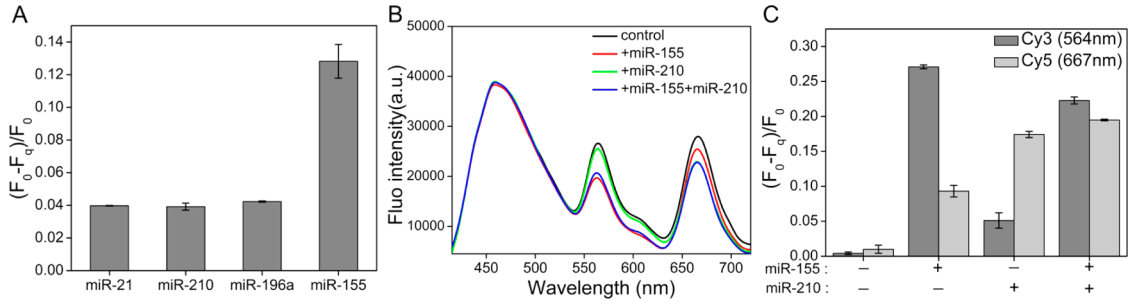

Figure 3. (A) Fluorescence intensity changes of different miRNAs (with a final concentration of 200 nM for miR-155 and 1 μM for miR-21, miR-210, and miR-196a). (B) Fluorescent spectra of multiple detection for miR-155 and miR-210 (with a final concentration of 200 nM each). (C) Representative fingerprint-like spectrum for the detection of different kind of miRNAs.

shown in Figure 1). Moreover, because of the intrinsic merits of MB probes (including predictable design, reproducibility of synthesis, and simplicity of modification) and the FRET signal transduction strategy of our design, the detection platform could be extended for detection of many other targets by changing the loop sequences of our probes, such as aptamers, DNAaymes, peptides, and metal ions.[19]

We first synthesized the GQDs as previous reported.[20] From Figure S1, we could see that the height of the synthesized GQDs was about 0.6−2 nm, suggesting 1−3 layers of graphene, and the diameters of GQDs were mainly distributed in a narrow range from 2 to 5 nm. Then, in order to characterize the FRET design, we incubated GQDs (with a final fixed concentration of 1.0 μg mL^{-1}) with a series of Cy3 labeled py-MB$_{155}$ probes (with different concentrations from 100 nM to 500 nM) to investigate the FRET efficacy. Through the typical excitation and emission spectra of Cy3 labeled py-MB$_{155}$ probes shown in Figure S3A, we could see that the optimal excitation wavelength of Cy3 was ∼550 nm, while excitation of 400 nm could not cause much emission of Cy3 comparing with 550 nm. As shown in Figure S2A, comparing to py-MBs themselves, an obvious fluorescent increase in the emission of labeled Cy3 (567 nm) under the excitation wavelength of GQDs (400 nm) was observed, which indicated that GQDs and the py-MBs were close proximity to generate FRET via the introduction of pyrene. Through calculation of the relative fluorescent intensity changes (ΔF) of Cy3, we found that 1.0 μg mL^{-1} of GQDs and 300 nM of py-MB$_{155}$ system has the highest ΔF (Figure S2B). Therefore, they were chosen as the optimal concentrations and used in further experiments.

We then evaluated the feasibility of combining the GQDs and py-MBs as a fluorescent biosensor platform for miRNA detection by using a DNA oligonucleotide (DNA $_{155}$) as a model system, whose sequence was the same with miR-155. Seen from Figure 2A, we observed an obvious increase of the fluorescent intensity of Cy3 (∼95% fluorescence augment) and a slight decrease of GQDs, which was due to the energy transfer from the photoexcited donor GQDs to the acceptor Cy3, causing the strong emission of Cy3 under the excitation wavelength of GQDs (400 nm). Meanwhile, the fluorescent intensity of Cy3 did not change much while there was only py-MB probe and DNA target, which indicated that GQDs, as photoexcited donors were essential to construct the detection platform. However, after adding DNA$_{155}$ targets (200 nM), an obvious decrease in the fluorescent intensity of Cy3 and a slight recovery of the fluorescence of GQDs were observed, which indicated that the hybridization between the probe and DNA$_{155}$ led to the conformation change of the probes, which significantly hindered FRET, resulting in 77% fluorescence decrease of Cy3. Therefore, we believed that our strategy was successful and this special fluorescent intensity change could be used for miRNA detection.

Recently, researches showed that the changes of miRNAs expression levels were associated with the tumor burden and malignant progression,[21] which demonstrated that miRNAs could play a very important role in the diagnosis of various cancers, such as lung cancer, pancreatic cancer.[22] So far, miRNAs have become clinically important biomarkers for early cancer diagnostic and prognostic processes.[23] Based on the above research, we then explored the platform as a sensitive biosensor for miRNA analysis. As illustrated in Figure 2B, the fluorescence intensity of Cy3 labeled on py-MB$_{155}$ decreased with the addition of miR-155 in a concentration-dependent way, which was mainly due to large amount of the duplex structures formed by the probes and miRNAs, thus hindered the FRET. The linear relationship between the relative fluorescence intensity change ΔF_r ($(F_0 - F_q)/F_0$) and the concentration of miR-155 was shown in Figure 2C, where F_0 is the fluorescence intensity of the Cy3 dye before hybridization with miRNA, and F_q is the corresponding fluorescence intensity after hybridization with different concentrations of miR-155. The linear equation was $y = 0.00159x + 0.03097$ with $R^2 = 0.9865$, which indicated that this method had a broad linear range from 0.1 to 200 nM with a detection limit of 100 pM (>3 standard deviations).

Next, we investigated the specificity of this biosensor, where four kinds of miRNA, including perfectly complementary target (miR-155) and three kinds of other miRNA (miR-21, miR-210, and miR-196a) were employed. As shown in Figure 3A, there were not obvious relative fluorescence intensity changes of other miRNAs comparing to the target miR-155, even with 5 times higher concentration (1 μM/200 nM). These results indicated that this novel fluorescent biosensor exhibited high selectivity toward different miRNA targets.

Multiple biomarker detection has been proved quite valuable for the early detection of cancer.[24] Toward this goal, we designed two different probes (py-MB$_{155}$ and py-MB$_{210}$) labeled with Cy3 and Cy5 for simultaneous detection of miR-155 and miR-210 respectively, where the selected two dyes and GQDs could trigger significant cascade FRET. The cascade FRET process was as followings: under the excitation wavelength of 400 nm, GQDs were excited and given emission wavelengths which could excite Cy3 dyes to give emission wavelengths used for exciting Cy5 dyes. In the multiple detection system, GQDs acted as donors for two dyes (Cy3, Cy5), and Cy3 acted as acceptors of GQDs but also as donors

DOI: 10.1021/acsami.5b04773
ACS Appl. Mater. Interfaces 2015, 7, 16152−16156

for Cy5. Meanwhile, as shown in Figure S3B, the optimal excitation wavelength of Cy5 was ~650 nm, while excitation of 400 nm could not cause much emission of Cy5. When the targets were added, the hybrid of duplex structures between probes and the targets formed, which caused fluorescence intensity changes of the dyes labeled on the corresponding probes and revealed the presence of the target. As shown in Figure 3B, when the target miR-155 existed, the fluorescence intensity of Cy3 labeled on the py-MB_{155} probe significantly decreased, and meanwhile the intensity of Cy5 slightly reduced. We ascribed that to the dual function of Cy3, who acted as acceptors for GQDs and donors for Cy5. When the target miR-210 existed, the strong hybridization interaction between py-MB_{210} and miR-210 caused the fluorescence intensity of Cy5 decreasing significantly. Meanwhile, when the two targets coexisted at the same time, the fluorescent intensities of both Cy3 and Cy5 decreased greatly. Therefore, as shown in Figure 3C, different targets resulted in differential fingerprint-like spectra, through which we obtained unique ΔF_r $((F_0 - F_q)/F_0)$ patterns with unique fingerprint features that could be employed for discrimination of miRNAs, and also for multiple detection.

3. CONCLUSION

In this work, we have demonstrated a novel fluorescent biosensor platform based on GQDs and py-MBs, which could be used for quantitative detection of miRNAs. The platform was elaborately designed, where pyrene and fluorescent dye dual labeled MBs were employed to strongly adsorb on the surface of GQDs via $\pi-\pi$ interactions, triggering FRET and generating fluorescent intensity changes as signals for target miRNA detection. This biosensor platform exhibited high specificity, good stability, and wide detection range (from 0.1 nM to 200 nM) with a lower detection limit of 100 pM. Moreover, considering of the large flexibility and high programmability of our platform, it opened a new gate for small nucleic acid molecular detection based on GQDs, even multiple detection. Therefore, we hope that the novel biosensor could provide new opportunities for early detection of cancer related biomarkers and for clinical diagnosis.

■ ASSOCIATED CONTENT

Supporting Information

The Supporting Information is available free of charge on the ACS Publications website at DOI: 10.1021/acsami.5b04773.

Sequences of the oligonucleotides and miRNAs used in this study, detailed experimental procedures, and optimization of the experimental conditions (PDF)

■ AUTHOR INFORMATION

Corresponding Authors

*E-mail: mixq@sari.ac.cn.

*E-mai: zuoxiaolei@sinap.ac.cn

Author Contributions

†H.Z., Y.W., and D.Z. contributed equally.

Notes

The authors declare no competing financial interest.

■ ACKNOWLEDGMENTS

This work was supported by Shanghai Municipal Science and Technology Commission (13DZ1940200, 15441905000), the National Natural Science Foundation of China (11405013), and Shanghai Yang Fan Plan (Grant 15YF1413300). A.A. acknowledges the financial support by Deanship of Scientific Research, College of Science Research Center, King Saud University.

■ REFERENCES

(1) Tan, W. H.; Wang, K. M.; Drake, T. J. Molecular Beacons. *Curr. Opin. Chem. Biol.* **2004**, *8*, 547−553.

(2) Xu, J. J.; Zhao, W. W.; Song, S. P.; Fan, C. H.; Chen, H. Y. Functional Nanoprobes for Ultrasensitive Detection of Biomolecules: an Update. *Chem. Soc. Rev.* **2014**, *43*, 1601−1611.

(3) Broude, N. E. Stem-loop Oligonucleotides: a Robust Tool for Molecular Biology and Biotechnology. *Trends Biotechnol.* **2002**, *20*, 249−256.

(4) Wang, J.; Chen, J. Y.; Chang, P.; LeBlanc, A.; Li, D. H.; Abbruzzesse, J. L.; Frazier, M. L.; Killary, A. M.; Sen, S. MicroRNAs in Plasma of Pancreatic Ductal Adenocarcinoma Patients as Novel Blood-Based Biomarkers of Disease. *Cancer Prev. Res.* **2009**, *2*, 807−813.

(5) Stobiecka, M.; Chalupa, A. Biosensors Based on Molecular Beacons. *Chem. Pap.* **2015**, *69*, 62−76.

(6) Wang, K. M.; Tang, Z. W.; Yang, C. Y. J.; Kim, Y. M.; Fang, X. H.; Li, W.; Wu, Y. R.; Medley, C. D.; Cao, Z. H.; Li, J.; Colon, P.; Lin, H.; Tan, W. H. Molecular Engineering of DNA: Molecular Beacons. *Angew. Chem., Int. Ed.* **2009**, *48*, 856−870.

(7) Wang, D.; Wang, L.; Dong, X. Y.; Shi, Z.; Jin, J. Chemically Tailoring Graphene Oxides into Fluorescent Nanosheets for Fe^{3+} Ion Detection. *Carbon* **2012**, *50*, 2147−2154.

(8) Zhou, X. J.; Zhang, Y.; Wang, C.; Wu, X. C.; Yang, Y. Q.; Zheng, B.; Wu, H. X.; Guo, S. W.; Zhang, J. Y. Photo-Fenton Reaction of Graphene Oxide: A New Strategy to Prepare Graphene Quantum Dots for DNA Cleavage. *ACS Nano* **2012**, *6*, 6592−6599.

(9) Gupta, V.; Chaudhary, N.; Srivastava, R.; Sharma, G. D.; Bhardwaj, R.; Chand, S. Luminscent Graphene Quantum Dots for Organic Photovoltaic Devices. *J. Am. Chem. Soc.* **2011**, *133*, 9960−9963.

(10) Shen, J. H.; Zhu, Y. H.; Yang, X. L.; Li, C. Z. Graphene Quantum Dots: Emergent Nanolights for Bioimaging, Sensors, Catalysis and Photovoltaic Devices. *Chem. Commun.* **2012**, *48*, 3686−3699.

(11) Zhu, S. J.; Zhang, J. H.; Qiao, C. Y.; Tang, S. J.; Li, Y. F.; Yuan, W. J.; Li, B.; Tian, L.; Liu, F.; Hu, R.; Gao, H. N.; Wei, H. T.; Zhang, H.; Sun, H. C.; Yang, B. Strongly Green-Photoluminescent Graphene Quantum Dots for Bioimaging Applications. *Chem. Commun.* **2011**, *47*, 6858−6860.

(12) Zhao, H. M.; Chang, Y. Y.; Liu, M.; Gao, S.; Yu, H. T.; Quan, X. A Universal Immunosensing Strategy Based on Regulation of the Interaction Between Graphene and Graphene Quantum Dots. *Chem. Commun.* **2013**, *49*, 234−236.

(13) He, S. J.; Song, B.; Li, D.; Zhu, C. F.; Qi, W. P.; Wen, Y. Q.; Wang, L. H.; Song, S. P.; Fang, H. P.; Fan, C. H. A Graphene Nanoprobe for Rapid, Sensitive, and Multicolor Fluorescent DNA Analysis. *Adv. Funct. Mater.* **2010**, *20*, 453−459.

(14) Wang, Y.; Li, Z. H.; Wang, J.; Li, J. H.; Lin, Y. H. Graphene and Graphene Oxide: Biofunctionalization and Applications in Biotechnology. *Trends Biotechnol.* **2011**, *29*, 205−212.

(15) Zhu, Y. W.; Murali, S.; Cai, W. W.; Li, X. S.; Suk, J. W.; Potts, J. R.; Ruoff, R. S. Graphene and Graphene Oxide: Synthesis, Properties, and Applications. *Adv. Mater.* **2010**, *22*, 5226−5226.

(16) Chen, Q. S.; Wei, W. L.; Lin, J. M. Homogeneous Detection of Concanavalin A Using Pyrene-Conjugated Maltose Assembled Graphene Based on Fluorescence Resonance Energy Transfer. *Biosens. Bioelectron.* **2011**, *26*, 4497−4502.

(17) Petrov, P. D.; Georgiev, G. L.; Muller, A. H. E. Dispersion of Multi-walled Carbon Nanotubes with Pyrene-Functionalized Polymeric Micelles in Aqueous Media. *Polymer* **2012**, *53*, 5502−5506.

(18) Zhang, Y. H.; Liu, C. J.; Shi, W. Q.; Wang, Z. Q.; Dai, L. M.; Zhang, X. Direct Measurements of the Interaction Between Pyrene

DOI: 10.1021/acsami.5b04773
ACS Appl. Mater. Interfaces 2015, 7, 16152−16156

and Graphite in Aqueous Media by Single Molecule Force Spectroscopy: Understanding the π-π Interactions. *Langmuir* **2007**, *23*, 7911−7915.
(19) Zheng, J.; Yang, R.; Shi, M.; Wu, C.; Fang, X.; Li, Y.; Li, J.; Tan, W. Rationally Designed Molecular Beacons for Bioanalytical and Biomedical Applications. *Chem. Soc. Rev.* **2015**, *44*, 3036−3055.
(20) Dong, Y. Q.; Shao, J. W.; Chen, C. Q.; Li, H.; Wang, R. X.; Chi, Y. W.; Lin, X. M.; Chen, G. N. Blue Luminescent Graphene Quantum Dots and Graphene Oxide Prepared by Tuning the Carbonization Degree of Citric Acid. *Carbon* **2012**, *50*, 4738−4743.
(21) Nicoloso, M. S.; Spizzo, R.; Shimizu, M.; Rossi, S.; Calin, G. A. MicroRNAs - the Micro Steering Wheel of Tumour Metastases. *Nat. Rev. Cancer* **2009**, *9*, 293−302.
(22) Lu, J.; Getz, G.; Miska, E. A.; Alvarez-Saavedra, E.; Lamb, J.; Peck, D.; Sweet-Cordero, A.; Ebet, B. L.; Mak, R. H.; Ferrando, A. A.; Downing, J. R.; Jacks, T.; Horvitz, H. R.; Golub, T. R. MicroRNA Expression Profiles Classify Human Cancers. *Nature* **2005**, *435*, 834−838.
(23) Chen, X.; Ba, Y.; Ma, L. J.; Cai, X.; Yin, Y.; Wang, K. H.; Guo, J. G.; Zhang, Y. J.; Chen, J. N.; Guo, X.; Li, Q. B.; Li, X. Y.; Wang, W. J.; Zhang, Y.; Wang, J.; Jiang, X. Y.; Xiang, Y.; Xu, C.; Zheng, P. P.; Zhang, J. B.; Li, R. Q.; Zhang, H. J.; Shang, X. B.; Gong, T.; Ning, G.; Wang, J.; Zen, K.; Zhang, J. F.; Zhang, C. Y. Characterization of MicroRNAs in Serum: a Novel Class of Biomarkers for Diagnosis of Cancer and Other Diseases. *Cell Res.* **2008**, *18*, 997−1006.
(24) Sidransky, D. Nucleic Acid-Based Methods for the Detection of Cancer. *Science* **1997**, *278*, 1054−1058.

DOI: 10.1021/acsami.5b04773
ACS Appl. Mater. Interfaces 2015, 7, 16152−16156